Trajectory tracking of a mini four-rotor helicopter in dynamic environments - a linear algebra approach

Claudio Rosales, Daniel Gandolfo, Gustavo Scaglia, Mario Jordan and Ricardo Carelli

Robotica / *FirstView* Article / April 2014, pp 1 - 25
DOI: 10.1017/S0263574714000952, Published online: 25 April 2014

Robotica: page 1 of 25. © Cambridge University Press 2014
doi:10.1017/S0263574714000952

Trajectory tracking of a mini four-rotor helicopter in dynamic environments - a linear algebra approach.

Claudio Rosales†*, Daniel Gandolfo†,
Gustavo Scaglia†, Mario Jordan‡ and Ricardo Carelli†

†*Instituto de Automática (INAUT), Universidad Nacional de San Juan, Avda. San Martín (oeste) 1109, CP 5400, San Juan - Argentina*
‡*Instituto Argentino de Oceanografía (IADO-CONICET) Florida 8000, Complejo CRIBABB, Edificio E1, Bahía Blanca B8000FWD Argentina*

(Accepted March 17, 2014)

SUMMARY
This paper presents the design of a controller that allows a four-rotor helicopter to track a desired trajectory in 3D space. To this aim, a dynamic model obtained from Euler-Lagrange equations describes the robot. This model is represented by numerical methods, with which the control actions for the operation of the system are obtained. The proposed controller is simple and presents good performance in face of uncertainties in the model of the system to be controlled. Zero-convergence proof is included, and simulation results show a good performance of the control system.

KEYWORDS: Trajectory tracking; Quadrotor; Numerical methods; Linear algebra.

1. Introduction

In past decades, the research effort on Unmanned Aerial Vehicles (UAV) has grown substantially, aimed at either military or civil applications, such as inspection of large areas in public safety applications,[18] natural risk management, cooperative transportation of payload with multiple aircraft,[19] inspection services of power lines,[16] photogrammetry,[12] intervention in hostile environments, infrastructure maintenance and precision agriculture.[13,14] In such cases, using UAV is extremely advantageous when compared to using one or several Unmanned Ground Vehicles (UGV), on account of its 3D mobility.

Unmanned aerial vehicles can be classified as fixed-wing, rotating-wing and blimps. The main advantage of rotating-wing over fixed-wing aircraft is the ability of hovering and having omnidirectional movement. However, one disadvantage is a relatively higher power consumption during flight. Within the rotating-wing aircraft classification, a quadrotor is much simpler and easier to build in comparison to a classical helicopter, because it has no swashplate and it is controlled by varying only the angular velocity of each one of the four motors.

According to ref. [2], two approaches can be adopted to model a miniature helicopter which is the UAV used in this work: a model based on physical equations, and a model based on system identification. The first one uses the motion equations to represent the physical system, the second one estimates the dynamic model of the physical system based on the data corresponding to its response to well-known input excitation. It is worth mentioning that such approaches are not mutually exclusive, and sometimes to use one to complement the other is a common practice.[11,27]

The control of quadrotor helicopters has attracted the attention of many researchers in the past few years. In the bibliography, different control strategies have been proposed, some of which use linearization techniques.[3,29] In ref. [5] a system model with DC motors and the use of the Lyapunov

* Corresponding author. E-mail: crosales@inaut.unsj.edu.ar

Function non-linear control technique for stabilizing aircraft orientation is presented, including a comparison of the real system's behaviour with the corresponding simulation. In ref. [6] the authors extend their work on the OS4 project as they compare classical PD and PID controllers for orientation stabilization with modern LQ adaptive optimal control, despite realizing that the latter one yields only an average result, due to modeling errors.

A meticulous study on the usually disregarded effects, such as blade flapping and propeller modeling, was developed in ref. [20]. In ref. [21], the authors continue to their work of implementing a X-4 flyer Mark II quadrotor by designing a discrete-time PID control law for their model including swift blade flapping dynamics. The closed-loop behaviour, though, turned out to be poor by unstability at high angular speed, which was attributed to high-frequency noise from the rotor interfering the accelerometer's reading. In ref. [4], the authors obtained a propulsion model that was included in the control scheme. From experimental results with helicopters and quadrotors, they also concluded that the aerodynamic force and torque for VTOL-robots under 20kg, can be approximated with simple algebraic equations.

In ref. [7], a real-time non-linear nested saturation control scheme based on Lyapunov's stability criterion is proposed, where each system state is sequentially stabilized through a wider stability region and, therefore, it achieve more aggressive maneuvering while maintaining good disturbance rejection. Later in ref. [9], the authors compared the performance of their non-linear control with a linear one LQR, which presents stability issues when the system is taken far away from the operation point chosen for controller design. It is worthwhile mentioning that Euler-Lagrange equations were used for modeling the miniature helicopter. Other proposals use backstepping techniques, as in refs. [10, 17].

This paper presents a control technique capable following piecewise continuous trajectories with piecewise continuous derivatives. It is a new control approach whose originality is based on applying numerical methods and linear algebra for trajectory tracking of a quadrotor. This simple approach suggests that, by knowing the value of the desired state, one can find a value for the control action which commands the system to move from its current state to the desired one. The main contribution of this work is that the proposed methodology is based on easily understandable concepts, requiring only basic knowledge of linear algebra and numerical methods. Therefore the controller is easy to manage for most designers, as compared to other controller proposals that need more complex mathematical tools.[10,22] Also, in comparison with other proposals,[1,30] the controller needs only basic algebra operations and to solve a system of linear equations on each sampling period, thus avoiding complex calculations. This makes the algorithm advantageous for on-board applications with reduced computational capability. The main advantage of this approach is controller simplicity, and the use of discrete-time equations, which turns very simple its implementation on a computer system.

The methodology is based on defining the reference trajectory in terms of a subset of state variables, and on determining the desired time-varying values for the remaining states. These state variables are found by analyzing the conditions for a system of linear equations to obtain an exact solution. Therefore, the control signals are obtained by solving a linear equations system. In refs. [23, 24, and 25], the numerical method based controller is introduced, where the control law depends on the chosen numerical approximation. This controller allows for achieving trajectory tracking control as well as positioning control, because it only depends on the reference values. A zero-convergence proof of the tracking error is also included.

The paper is organized as follows: in Section 2, the dynamic model of a four rotors helicopter is presented. In Section 3, the helicopter model is approached by using numerical methods and the expression of the proposed controller is obtained. In Section 4, simulation results of the control algorithm validate the theoretical results and show the characteristics of the proposed controller. In Section 5, the conclusions of the paper and proposals for future work are presented.

2. Dynamic Model of a Quadrotor

In this section, the dynamic model of the four-rotor helicopter using Euler-Lagrange equations is obtained. This was described in ref. [8]. The generalized coordinates of the aircraft are:

$$q = (x, y, z, \phi, \theta, \psi) \, \epsilon \Re^6 \tag{1}$$

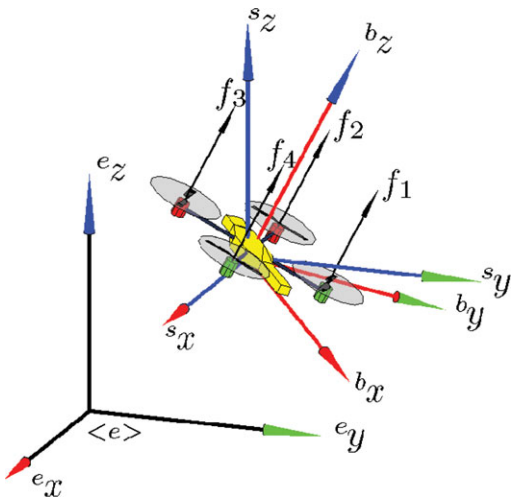

Fig. 1. (Colour online) Diagram of a 6-DOF quadrotor. The associated frames e_i, s_i and b_i represent the inertial, spatial and body frame, respectively.

where $\xi = (x, y, z)$ denotes the position of center of mass of the helicopter related to the inertial frame $\langle e \rangle$, and $\eta = (\phi, \theta, \psi) \epsilon\ \Re^3$ are the Euler angles, ϕ is the roll angle, θ is the pitch angle and ψ is the yaw angle in the spatial frame $\langle s \rangle$, all of which t represents the helicopter orientation (See Fig. 1). By defining the Lagrangian:

$$L_{(q,\dot{q})} = T_{trans} + T_{rot} - U \tag{2}$$

where $T_{trans} = \frac{m}{2}\dot{\xi}^T\dot{\xi}$ is the translational kinetic energy, $T_{rot} = \frac{1}{2}\omega^T I\omega$ is the rotational kinetic energy, $U = mgz$ is the potential energy of the system, z is the vehicle height, m denotes the helicopter mass, ω is the angular velocity, I is the inertia matrix and g is the gravitational acceleration. The angular velocity vector ω with respect to the body frame relates to the generalized velocities (where the Euler angles are valid) using a standard kinematic relation.

$$\dot{\eta} = W_\eta^{-1}\omega \tag{3}$$

where

$$W_\eta = \begin{bmatrix} 1 & 0 & -\sin\theta \\ 0 & \cos(\psi) & \cos\theta\sin\psi \\ 0 & \sin(\psi) & \cos\theta\cos\psi \end{bmatrix} \tag{4}$$

By establishing,

$$J = J_{(\eta)} = W_\eta^T I W_\eta \tag{5}$$

Such that,

$$T_{rot} = \frac{1}{2}\dot{\eta}^T J\dot{\eta} \tag{6}$$

The matrix J acts as an inertia matrix for the total rotational kinetic energy of the helicopter expressed in terms of generalized coordinates η. The entire dynamic model of the helicopter is obtained from Euler-Lagrange equations with external generalized forces:

$$\frac{d}{dt}\frac{\partial L}{\partial \dot{q}} - \frac{\partial L}{\partial q} = \begin{bmatrix} F_\xi \\ \tau \end{bmatrix} \tag{7}$$

where $F_\xi = RF \epsilon \Re^3$ is the translational force applied to the vehicle, which is caused by the main control input. R is a rotational matrix $R(\phi, \theta, \psi)$ that represents the orientation of the quadrotor relative to inertial frame, while $\tau \epsilon \Re^3$ represents the moment of pitch, roll and yaw. The principal input of the aircraft is the impulse of the four propellers,

$$F = \begin{bmatrix} 0 \\ 0 \\ u \end{bmatrix} \tag{8}$$

where,

$$u = f_1 + f_2 + f_3 + f_4 \tag{9}$$

and from,[15]

$$f_i = k_i \omega_i^2 \quad \text{for } i = 1, \ldots, 4 \; k_i > 0 \tag{10}$$

Parameter k_i is taken as a constant value and ω_i is the angular velocity of the $i - th$ motor. The generalized torques are:

$$\tau = \begin{bmatrix} \tau_\phi \\ \tau_\theta \\ \tau_\psi \end{bmatrix} \triangleq \begin{bmatrix} (f_3 - f_1)l \\ (f_2 - f_4)l \\ \sum_{i=0}^{4} \tau_{Mi} \end{bmatrix} \tag{11}$$

where l is the distance separating the motors from the gravity center, and τ_{Mi} is the torque caused by the motor M_i, $i = 1, \ldots, 4$ about the center of gravity of the helicopter. Because the Lagrangian does not show any term in the kinematic energy which combines $\dot{\xi}$ with $\dot{\eta}$, the Euler-Lagrange equations can be broken down in dynamics for the coordinates ξ and the coordinates η.

$$m\ddot{\xi} + \begin{bmatrix} 0 \\ 0 \\ mg \end{bmatrix} = F_\xi \tag{12}$$

$$J\ddot{\eta} + \dot{J}\dot{\eta} - \frac{1}{2}\frac{\partial}{\partial \eta}(\dot{\eta}^T J \dot{\eta}) = \tau \tag{13}$$

By defining the terms of Coriolis that represents the gyroscope and centrifugal effects associated with η as,

$$C_{(\eta,\dot{\eta})}\dot{\eta} = \dot{J}\dot{\eta} - \frac{1}{2}\frac{\partial}{\partial \eta}(\dot{\eta}^T J \dot{\eta}) \tag{14}$$

and,

$$\begin{gathered} m\ddot{\xi} + \begin{bmatrix} 0 \\ 0 \\ mg \end{bmatrix} = F_\xi \\ J\ddot{\eta} + C_{(\eta,\dot{\eta})}\dot{\eta} = \tau \end{gathered} \tag{15}$$

From[8] and aiming at simplifying the model, the following change in the input variable is proposed:

$$\tau = C_{(\eta,\dot{\eta})}\dot{\eta} + J\tilde{\tau} \tag{16}$$

where $\tilde{\tau} = [\tilde{\tau_\phi}, \tilde{\tau_\theta}, \tilde{\tau_\psi}]$, is the new input vector. Then,

$$\ddot{\eta} = \tilde{\tau} \tag{17}$$

Thus obtaining:

$$\begin{aligned} m\ddot{x} &= -u\sin\theta \\ m\ddot{y} &= u\cos\theta\sin\phi \\ m\ddot{z} &= u\cos\theta\cos\phi - mg \\ \ddot{\phi} &= \tilde{\tau}_{\phi} \\ \ddot{\theta} &= \tilde{\tau}_{\theta} \\ \ddot{\psi} &= \tilde{\tau}_{\psi} \end{aligned} \tag{18}$$

where x and y are the coordinates on the horizontal plane, z is the vertical position, and $\tilde{\tau_{\phi}}$, $\tilde{\tau_{\theta}}$ and $\tilde{\tau_{\psi}}$ are the roll, pitch and yaw torques, respectively, which are related to the generalized torques τ_{ϕ}, τ_{θ} and τ_{ψ} through Eq. (16).

3. Controller Design

3.1. Problem statement

Let us consider the following differential equation,

$$\dot{y} = f_{(y,t)} \quad y_{(0)} = y_0 \tag{19}$$

aimed at determining the value of $y_{(t)}$ in discrete time instants $t = nT_o$, where T_o is the sample time and $n \epsilon \{0, 1, 2, 3, \ldots\}$. Variable $y_{(t)}$ for $t = nT_o$, will be symbolized as $y_{(n)}$. Thus, if needing to calculate $y_{(n+1)}$ with the known value of $y_{(n)}$, Eq. (19) should be integrated for the interval $nT_o \leqslant t \leqslant (n+1)T_o$, as

$$y_{(n+1)} = y_{(n)} + \int_{nT_o}^{(n+1)T_o} f_{(y,t)}dt \tag{20}$$

An approximate value of $y_{(n+1)}$ can be obtained using numerical methods by integrating the right-hand member of (20). For instance, it can be calculated as,

$$y_{(n+1)} \cong y_{(n)} + T_o f_{(y_{(n)}, t_{(n)})} \tag{21}$$

which is called the Euler approximation. Even though there are other numerical methods for approximating the integral in Eq. (20), here Euler approximation is applied to obtain the discrete dynamic model of a quadrotor. Based on this model, the optimal control actions that allow the helicopter to follow a previously established path will be obtained, by ultimately solving a least squares algebraic problem.

3.2. Controller design

In this section, a control law is designed capable of generating the signals $[u, \tilde{\tau_{\phi}}, \tilde{\tau_{\theta}}, \tilde{\tau_{\psi}}]$, with the goal of making, helicopter position $[X_{(t)}, Y_{(t)}, Z_{(t)}, \Psi_{(t)}]$ follow the desired trajectory

$[X_{d_{(t)}}, Y_{d_{(t)}}, Z_{d_{(t)}}, \Psi_{d_{(t)}}]$. The relationship between the generalized pairs and the new inputs $(\tilde{\tau})$ is given in (16).

The first step in controller design involves expressing the model of (18) in state form as a set of linear first-order differential equations,

$$\begin{bmatrix} \dot{x_1} \\ \dot{x_2} \\ \dot{x_3} \\ \dot{x_4} \\ \dot{x_5} \\ \dot{x_6} \\ \dot{x_7} \\ \dot{x_8} \\ \dot{x_9} \\ \dot{x_{10}} \\ \dot{x_{11}} \\ \dot{x_{12}} \end{bmatrix} = \begin{bmatrix} x_2 \\ -\frac{u}{m}\sin x_9 \\ x_4 \\ \frac{u}{m}\cos x_9 \sin x_7 \\ x_6 \\ \frac{u}{m}\cos x_9 \cos x_7 - g \\ x_8 \\ \tilde{\tau}_\phi \\ x_{10} \\ \tilde{\tau}_\theta \\ x_{12} \\ \tilde{\tau}_\psi \end{bmatrix} \text{ where } \begin{bmatrix} x \\ \dot{x} \\ y \\ \dot{y} \\ z \\ \dot{z} \\ \phi \\ \dot{\phi} \\ \theta \\ \dot{\theta} \\ \psi \\ \dot{\psi} \end{bmatrix} = \begin{bmatrix} x_1 \\ x_2 \\ x_3 \\ x_4 \\ x_5 \\ x_6 \\ x_7 \\ x_8 \\ x_9 \\ x_{10} \\ x_{11} \\ x_{12} \end{bmatrix} \tag{22}$$

Through Euler approximation, whose results are

$$\begin{aligned}
x_{1_{(n+1)}} &= x_{1_{(n)}} + x_{2_{(n)}} T_o \\
x_{2_{(n+1)}} &= x_{2_{(n)}} - \frac{u_{(n)}}{m} \sin x_{9_{(n)}} T_o \\
x_{3_{(n+1)}} &= x_{3_{(n)}} + x_{4_{(n)}} T_o \\
x_{4_{(n+1)}} &= x_{4_{(n)}} + \frac{u_{(n)}}{m} \cos x_{9_{(n)}} \sin x_{7_{(n)}} T_o \\
x_{5_{(n+1)}} &= x_{5_{(n)}} + x_{6_{(n)}} T_o \\
x_{6_{(n+1)}} &= x_{6_{(n)}} + \frac{u_{(n)}}{m} \cos x_{9_{(n)}} \cos x_{7_{(n)}} T_o - g T_o \\
x_{7_{(n+1)}} &= x_{7_{(n)}} + x_{8_{(n)}} T_o \\
x_{8_{(n+1)}} &= x_{8_{(n)}} + \tilde{\tau}_{\phi(n)} T_o \\
x_{9_{(n+1)}} &= x_{9_{(n)}} + x_{10_{(n)}} T_o \\
x_{10_{(n+1)}} &= x_{10_{(n)}} + \tilde{\tau}_{\theta(n)} T_o \\
x_{11_{(n+1)}} &= x_{11_{(n)}} + x_{12_{(n)}} T_o \\
x_{12_{(n+1)}} &= x_{12_{(n)}} + \tilde{\tau}_{\psi(n)} T_o
\end{aligned} \tag{23}$$

If the desired trajectory were given, $[X_{d_{(n+1)}}, Y_{d_{(n+1)}}, Z_{d_{(n+1)}}, \Psi_{d_{(n+1)}}]^T$, then it could be taken into account for computing the required control action $[u, \tilde{\tau_\phi}, \tilde{\tau_\theta}, \tilde{\tau_\psi}]^T$, which allow, the helicopter to evolve from the present position to the desired trajectory.

By expressing (23) in matrix form and operating,

$$\underbrace{\begin{bmatrix} -\frac{To}{m}\sin x_{9_{(n)}} & 0 & 0 & 0 \\ \frac{To}{m}\cos x_{9_{(n)}}\sin x_{7_{(n)}} & 0 & 0 & 0 \\ \frac{To}{m}\cos x_{9_{(n)}}\cos x_{7_{(n)}} & 0 & 0 & 0 \\ 0 & T_o & 0 & 0 \\ 0 & 0 & T_o & 0 \\ 0 & 0 & 0 & T_o \\ 0 & 0 & 0 & 0 \\ 0 & 0 & 0 & 0 \\ 0 & 0 & 0 & 0 \\ 0 & 0 & 0 & 0 \\ 0 & 0 & 0 & 0 \\ 0 & 0 & 0 & 0 \end{bmatrix}}_{A} \underbrace{\begin{bmatrix} u_{(n)} \\ \tilde{\tau}_{\phi(n)} \\ \tilde{\tau}_{\theta(n)} \\ \tilde{\tau}_{\psi(n)} \end{bmatrix}}_{\mathbf{w}} = \underbrace{\begin{bmatrix} x_{2_{(n+1)}} - x_{2_{(n)}} \\ x_{4_{(n+1)}} - x_{4_{(n)}} \\ x_{6_{(n+1)}} - x_{6_{(n)}} + gT_o \\ x_{8_{(n+1)}} - x_{8_{(n)}} \\ x_{10_{(n+1)}} - x_{10_{(n)}} \\ x_{12_{(n+1)}} - x_{12_{(n)}} \\ x_{1_{(n+1)}} - x_{1_{(n)}} - T_o x_{2_{(n)}} \\ x_{3_{(n+1)}} - x_{3_{(n)}} - T_o x_{4_{(n)}} \\ x_{5_{(n+1)}} - x_{5_{(n)}} - T_o x_{6_{(n)}} \\ x_{7_{(n+1)}} - x_{7_{(n)}} - T_o x_{8_{(n)}} \\ x_{9_{(n+1)}} - x_{9_{(n)}} - T_o x_{10_{(n)}} \\ x_{11_{(n+1)}} - x_{11_{(n)}} - T_o x_{12_{(n)}} \end{bmatrix}}_{b} \tag{24}$$

or, in compact form as.

$$A\mathbf{w} = b \tag{25}$$

Equation (24) represents a system of linear equations which allows for calculating the control actions ($\mathbf{w}$) at each sampling time so that the quadrotor achieves the desired trajectory. Now, it is necessary to set the conditions for this system in order to have an exact solution. Then, the first condition for the system of (24) is that the system of 6 equations and 4 unknown variables in (26) have an exact solution.

$$\begin{bmatrix} -\frac{\sin x_{9_{(n)}}}{m} & 0 & 0 & 0 \\ \frac{\cos x_{9_{(n)}}\sin x_{7_{(n)}}}{m} & 0 & 0 & 0 \\ \frac{\cos x_{9_{(n)}}\cos x_{7_{(n)}}}{m} & 0 & 0 & 0 \\ 0 & 1 & 0 & 0 \\ 0 & 0 & 1 & 0 \\ 0 & 0 & 0 & 1 \end{bmatrix} \begin{bmatrix} u \\ \tilde{\tau}_{\phi} \\ \tilde{\tau}_{\theta} \\ \tilde{\tau}_{\psi} \end{bmatrix} = \begin{bmatrix} \frac{x_{2_{(n+1)}} - x_{2_{(n)}}}{T_o} \\ \frac{x_{4_{(n+1)}} - x_{4_{(n)}}}{T_o} \\ \frac{x_{6_{(n+1)}} - x_{6_{(n)}} + gT_o}{T_o} \\ \frac{x_{8_{(n+1)}} - x_{8_{(n)}}}{T_o} \\ \frac{x_{10_{(n+1)}} - x_{10_{(n)}}}{T_o} \\ \frac{x_{12_{(n+1)}} - x_{12_{(n)}}}{T_o} \end{bmatrix} \tag{26}$$

From (27) it can be concluded that these conditions are given as in (28) and (29).

$$\begin{bmatrix} -\frac{\sin x_{9_{(n)}}}{m} \\ \frac{\cos x_{9_{(n)}}\sin x_{7_{(n)}}}{m} \\ \frac{\cos x_{9_{(n)}}\cos x_{7_{(n)}}}{m} \end{bmatrix} [u] = \begin{bmatrix} \frac{x_{2_{(n+1)}} - x_{2_{(n)}}}{T_o} \\ \frac{x_{4_{(n+1)}} - x_{4_{(n)}}}{T_o} \\ \frac{x_{6_{(n+1)}} - x_{6_{(n)}} + gT_o}{T_o} \end{bmatrix} = \begin{bmatrix} \frac{\Delta x_2}{T_o} \\ \frac{\Delta x_4}{T_o} \\ \frac{\Delta x_6 + gT_o}{T_o} \end{bmatrix} \tag{27}$$

$$\tan x_{7_{ez}} = \frac{\Delta x_4}{\Delta x_6 + gT_o} \tag{28}$$

$$\tan x_{9_{ez}} = -\frac{\Delta x_2}{\Delta x_4}\sin x_{7_{ez}} \tag{29}$$

From (28) and (29), the variable references $x_{7_{ez}}$ and $x_{9_{ez}}$ are obtained so that the system of Eq. (24) have an exact solution and thus, the quadrotor can follow the reference trajectory. These variables

represent the necessary orientations to make the tracking error tend to zero, and the reference values for pitch ($x_{7_{ez}} = x_{7d_{(n+1)}}$) and roll ($x_{_{ez}} = x_{9d_{(n+1)}}$) angles as shown in appendix A.

In addition, from (24) it can be noted that, to make the equation system reach at an exact solution, the rows of b corresponding to the zero rows of A must be equal to zero. Then

$$\begin{bmatrix} x_{2_{(n)}} \\ x_{4_{(n)}} \\ x_{6_{(n)}} \\ x_{8_{(n)}} \\ x_{10_{(n)}} \\ x_{12_{(n)}} \end{bmatrix} = \frac{1}{T_o} \begin{bmatrix} x_{1ref(n+1)} - x_{1(n)} \\ x_{3ref(n+1)} - x_{3(n)} \\ x_{5ref(n+1)} - x_{5(n)} \\ x_{7ez} - x_{7(n)} \\ x_{9ez} - x_{9(n)} \\ x_{11ref(n+1)} - x_{11(n)} \end{bmatrix} \tag{30}$$

From the previous equations, the speed references that make the quadrotor follow the desired trajectory are obtained.

In order for the tracking error tend to zero, the following expressions are defined,

$$\begin{aligned} x_{1ref_{(n+1)}} &= x_{1d_{(n+1)}} - k_{x1}(x_{1d_{(n)}} - x_{1_{(n)}}) \\ x_{3ref_{(n+1)}} &= x_{3d_{(n+1)}} - k_{x3}(x_{3d_{(n)}} - x_{3_{(n)}}) \\ x_{5ref_{(n+1)}} &= x_{5d_{(n+1)}} - k_{x5}(x_{5d_{(n)}} - x_{5_{(n)}}) \\ x_{7ref_{(n+1)}} &= x_{7ez_{(n+1)}} - k_{x7}(x_{7ez_{(n)}} - x_{7_{(n)}}) \\ x_{9ref_{(n+1)}} &= x_{9ez_{(n+1)}} - k_{x9}(x_{9ez_{(n)}} - x_{9_{(n)}}) \\ x_{11ref_{(n+1)}} &= x_{11d_{(n+1)}} - k_{x11}(x_{11d_{(n)}} - x_{11_{(n)}}) \end{aligned} \tag{31}$$

where $0 < k_{x1}, k_{x3}, k_{x5}, k_{x7}, k_{x9}, k_{x11} < 1$.

When replacing (31) in (30), the velocities needed to make the tracking error tend to zero are obtained. These values are the desired values that enable follow the trajectory correctly, and denoted with the subscript "d".

$$\begin{aligned} x_{2d_{(n+1)}} &= \frac{(x_{1d(n+1)} - k_{x1}(x_{1d(n)} - x_{1(n)})) - x_{1(n)}}{T_o} \\ x_{4d_{(n+1)}} &= \frac{(x_{3d(n+1)} - k_{x3}(x_{3d(n)} - x_{3(n)})) - x_{3(n)}}{T_o} \\ x_{6d_{(n+1)}} &= \frac{(x_{5d(n+1)} - k_{x5}(x_{5d(n)} - x_{5(n)})) - x_{5(n)}}{T_o} \\ x_{8d_{(n+1)}} &= \frac{(x_{7ez(n+1)} - k_{x7}(x_{7ez(n)} - x_{7(n)})) - x_{7(n)}}{T_o} \\ x_{10d_{(n+1)}} &= \frac{(x_{9ez(n+1)} - k_{x9}(x_{9ez(n)} - x_{9(n)})) - x_{9(n)}}{T_o} \\ x_{12d_{(n+1)}} &= \frac{(x_{11d(n+1)} - k_{x11}(x_{11d(n)} - x_{11(n)})) - x_{11(n)}}{T_o} \end{aligned} \tag{32}$$

Similar approach as in (31) was used, with reference speed values obtained in (32) to make the speed quadrotor tend to the reference speed.

$$\begin{aligned}
x_{2ref_{(n+1)}} &= x_{2d_{(n+1)}} - k_{x2}(x_{2d_{(n)}} - x_{2_{(n)}}) \\
x_{4ref_{(n+1)}} &= x_{4d_{(n+1)}} - k_{x4}(x_{4d_{(n)}} - x_{4_{(n)}}) \\
x_{6ref_{(n+1)}} &= x_{6d_{(n+1)}} - k_{x6}(x_{6d_{(n)}} - x_{6_{(n)}}) \\
x_{8ref_{(n+1)}} &= x_{8d_{(n+1)}} - k_{x8}(x_{8d_{(n)}} - x_{8_{(n)}}) \\
x_{10ref_{(n+1)}} &= x_{10d_{(n+1)}} - k_{x10}(x_{10d_{(n)}} - x_{10_{(n)}}) \\
x_{12ref_{(n+1)}} &= x_{12d_{(n+1)}} - k_{x12}(x_{12d_{(n)}} - x_{12_{(n)}})
\end{aligned} \tag{33}$$

where $0 < k_{x2}, k_{x4}, k_{x6}, k_{x8}, k_{x10}, k_{x12} < 1$.

The final system to be solved is the following one:

$$\begin{bmatrix} -\frac{\sin x_{9ez(n)}}{m} & 0 & 0 & 0 \\ \frac{\cos x_{9ez(n)} \sin x_{7ez(n)}}{m} & 0 & 0 & 0 \\ \frac{\cos x_{9ez(n)} \cos x_{7ez(n)}}{m} & 0 & 0 & 0 \\ 0 & 1 & 0 & 0 \\ 0 & 0 & 1 & 0 \\ 0 & 0 & 0 & 1 \end{bmatrix} \begin{bmatrix} u \\ \tilde{\tau}_\phi \\ \tilde{\tau}_\theta \\ \tilde{\tau}_\psi \end{bmatrix} = \frac{1}{T_o} \begin{bmatrix} x_{2ref_{(n+1)}} - x_{2_{(n)}} \\ x_{4ref_{(n+1)}} - x_{4_{(n)}} \\ x_{6ref_{(n+1)}} - x_{6_{(n)}} + gT_o \\ x_{8ref_{(n+1)}} - x_{8_{(n)}} \\ x_{10ref_{(n+1)}} - x_{10_{(n)}} \\ x_{12ref_{(n+1)}} - x_{12_{(n)}} \end{bmatrix} = \frac{1}{To} \begin{bmatrix} \Delta x_2 \\ \Delta x_4 \\ \Delta x_6 + gT_o \\ \Delta x_8 \\ \Delta x_{10} \\ \Delta x_{12} \end{bmatrix} \tag{34}$$

Equation (34) is solved using the pseudo-inverse matrix, that allos, obtaining the control actions.

$$\mathbf{w} = A^{\dagger} b \tag{35}$$

Equation (35) represents the optimal least squares solution.[28] Columns of matrix A are linearly independent. Then, the solution of (34) can be expressed as,

$$\mathbf{w} = (A^T A)^{-1} A^T b \tag{36}$$

By developing the above expression,

$$(A^T A)^{-1} = \begin{bmatrix} m^2 & 0 & 0 & 0 \\ 0 & 1 & 0 & 0 \\ 0 & 0 & 1 & 0 \\ 0 & 0 & 0 & 1 \end{bmatrix} \tag{37}$$

and,

$$A^T b = \frac{1}{T_o} \begin{bmatrix} -\sin x_{9ez(n)} \frac{\Delta x_2}{m} + \cos x_{9ez(n)} \sin x_{7ez(n)} \frac{\Delta x_4}{m} + \cos x_{9ez(n)} \cos x_{7ez(n)} \frac{(\Delta x_6 + gT_o)}{m} \\ x_{8ref(n+1)} - x_{8(n)} \\ x_{10ref(n+1)} - x_{10(n)} \\ x_{12ref(n+1)} - x_{12(n)} \end{bmatrix} \tag{38}$$

Upon solving system (36), the expression for the control actions is found.

$$u = \frac{m}{T_o} \left(-\sin x_{9ez(n)} \Delta x_2 + \cos x_{9ez(n)} \sin x_{7ez(n)} \Delta x_4 + \cos x_{9ez(n)} \cos x_{7ez(n)} (\Delta x_6 + gT_o) \right) \tag{39}$$

$$\tilde{\tau}_\phi = \frac{x_{8ref(n+1)} - x_{8(n)}}{T_o} \tag{40}$$

$$\tilde{\tau}_\theta = \frac{x_{10ref(n+1)} - x_{10(n)}}{T_o} \tag{41}$$

$$\tilde{\tau}_\psi = \frac{x_{12ref(n+1)} - x_{12(n)}}{T_o} \tag{42}$$

Table I. Control gains used in the first simulation.

$k_{x1} = 0.78$	$k_{x2} = 0.8$
$k_{x3} = 0.77$	$k_{x4} = 0.8$
$k_{x5} = 0.9$	$k_{x6} = 0.95$
$k_{x7} = 0.7$	$k_{x8} = 0.67$
$k_{x9} = 0.7$	$k_{x10} = 0.67$
$k_{x11} = 0.8$	$k_{x12} = 0.85$

From (40), (41) and (42), and using Eq. (16), the real torques $[\tau_\phi, \tau_\theta, \tau_\psi]^T$ can be obtained. The control action u, can be applied to the vehicle whose model is expressed in (15).

4. Simulation Results

This subsection presents three flight 3D simulations with the quadrotor, using the controller designed in Section 3. The simulations are aimed at confirming an optimal performance of the control law. The first simulation shows the performance of the controller without model uncertainties and disturbance. The second simulation includes model parametric errors and measurement noise, and the last simulations display the performance of the controller for a square trajectory. The first simulation is performed using a simulator developed on Matlab© platform, which considers an accurate model of the vehicle. The values of the parameters of quadrotor models ((12) and (13)) are obtained from,[17]

$$\begin{array}{ccc} m = 0.5kg & l = 0.24m & g = 9.81m/s^2 \\ I = diag[3.8 & 3.8 & 7.1] * 10^{-3} Nms^2/rad \end{array}$$

In order to check the performance of the proposed controller, a helical path was used as the desired trajectory, centered at the origin of the inertial frame with radius $2m$ and the quadrotor orientation (Ψ_d) set to $\pi/2$ radians. In order to demonstrate that the proposed controller is also useful for position control, it is considered a reference point $(Xd, Yd, Zd, \Psi d) = (0m, 0m, 12m, -\pi/2rad)$, and a final motion to descend to the origin $(Xd, Yd, Zd, \Psi d) = (0m, 0m, 0m, 0rad)$ of the inertial frame to complete the simulation. The helical trajectory is generated with an upward velocity $v_z = 0.8m/s$ and an angular velocity $\omega = 1rad/s$. The initial helicopter position is located at the frame origin and the trajectory starts at position [0m ; 0m ; 2m]. A sample time of $50ms$ was used in simulations. The selected control gains are shown in Table I. The values of constants were chosen heuristically. To make the tracking errors tend to zero smoothly, constants k_{xi} have been introduced as design parameters, and in some way, they adjust the convergence rate of actual states to the desired states. It should be recalled that the constant values must be $0 < k_{xi} < 1$ with $i = 1, 2, \ldots, 12$, to ensure the convergence to zero of tracking errors. For values close to 0, the variables reach the references quickly, but it attains more abrupt responses whereas constants near to 1 cause soft responses but the reference is reached in a longer time. Therefore, the values of k_{xi}, associated to ϕ (roll) and θ (pitch) angles are lower than those of k_{xi}, associated to the remaining variables because it is necessary to reach these desired angles faster than the other remaining variables of the system. Besides, any $x - y$ position depends on these angles.

Figure 2 shows the 3D representation of the helicopter's position, which succeeds in reaching and following the desired trajectory. The evolution of the quadrotor to the desired set points during positioning control is also shown. Figure 3 shows the time evolution of coordinates x, y, z, which tend to the reference values. Figure 4 shows the time evolution of the attitude variables ϕ, θ and ψ, which also approximate their reference values. Figure 5 represents the control errors which tend to zero, including those of the position control phase. Finally, Fig. 6 represents the control actions $(u, \tau_\phi, \tau_\theta, \tau_\psi)$ expressed by (9) and (11), which are the real control actions directly applied to the vehicle. In the second experiment, the goal is to show the performance of the controller, including errors in the system parameters and measurement noise. The parameter error is estimated to be about 20 percent of the real value. Table II shows the parameter values considered for this simulation. White Gaussian noise was also added in the measurement of accelerations, averaging five percent of the

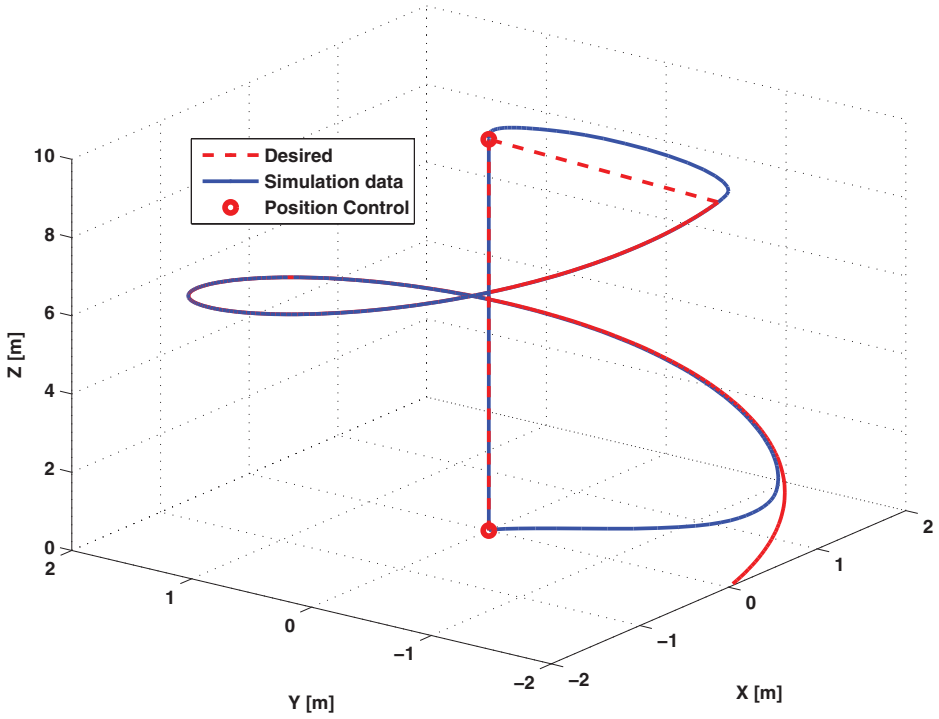

Fig. 2. (Colour online) Evolution of the quadrotor position.

Table II.

Controller parameters	Model parameters
$m = 0.6[kg]$	$m = 0.5[kg]$
$I_{xx} = 2.7 * 10^{-3} m/s^2$	$I_{xx} = 3.8 * 10^{-3} m/s^2$
$I_{yy} = 4.8 * 10^{-3} m/s^2$	$I_{yy} = 3.8 * 10^{-3} m/s^2$
$I_{zz} = 8.9 * 10^{-3} m/s^2$	$I_{xx} = 7.1 * 10^{-3} m/s^2$

measured values. This error affects the estimations speed and position measurements because they are obtained by integrating the acceleration readings.

Figure 7 the 3D evolution of the vehicle, where a steady-state error on z is noted. This is due to the error in mass parameter, which causes weight miscalculations by the controller. In spite of it, it is worth mentioning that the authors have always had a sound estimation of mass parameters in real applications. The performance of other controlled variables (x, y, ψ) are quite acceptable.

Figure 8 shows the time evolution of coordinates x, y, z with z showing a steady-state error, as denoted above. Figure 9 represents the time evolution of the attitude variables ϕ, θ and ψ of the quadrotor. These variables are less affected by parameter errors than the position variables. Figure 10 reveals the error evolution, which does not tend to zero but is very low. Finally, Figure 11 shows the control actions for this simulation. The variations in signal values at 12 and 25 seconds are explained by abrupt changes in the reference values for position control. At $t = 12$ seconds all references vary, but at 25 seconds only the vertical position and the yaw angle vary. The controller performance under parametric errors and measurement noise turns to be quite satisfactory, as noted from the figures.

In the last simulations, the objective is to demonstrate the management of corners for a square trajectory at constant altitude reference. The height is $5m$, and each of side is $5m$. This reference does not generate any mathematical singularity on the controller. As mentioned in Section 1, the presented control technique can follow piecewise continuous trajectories and piecewise continuous derivatives. The problem generated at corners are the sharp variations in reference, which cause large control errors, in turn generate large values of control actions that are impossible to reach, due to

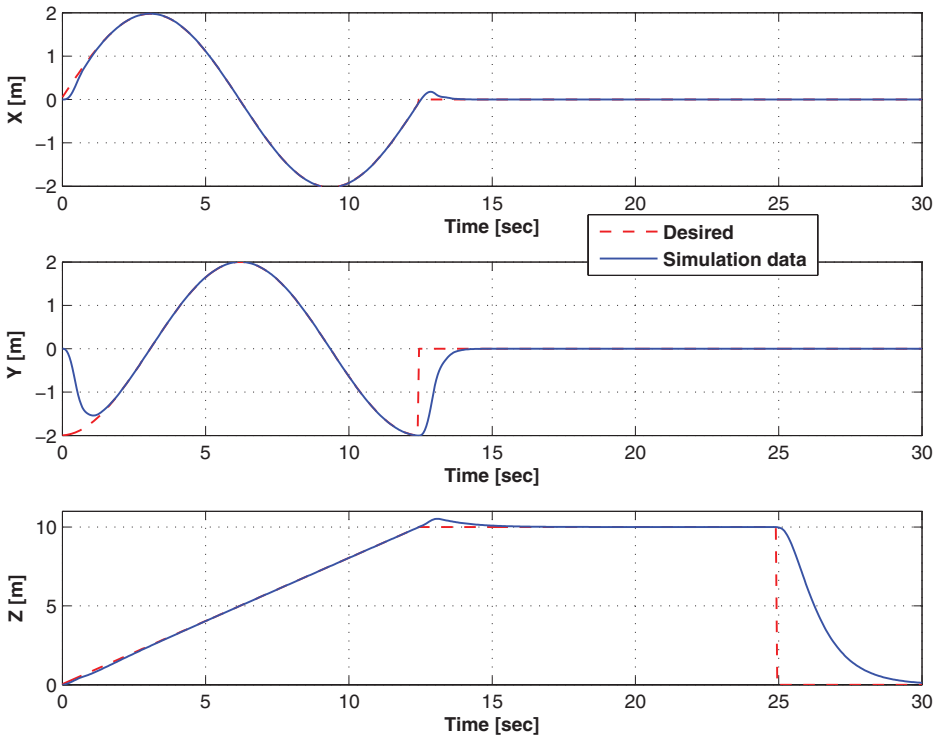

Fig. 3. (Colour online) Time evolution of position variables.

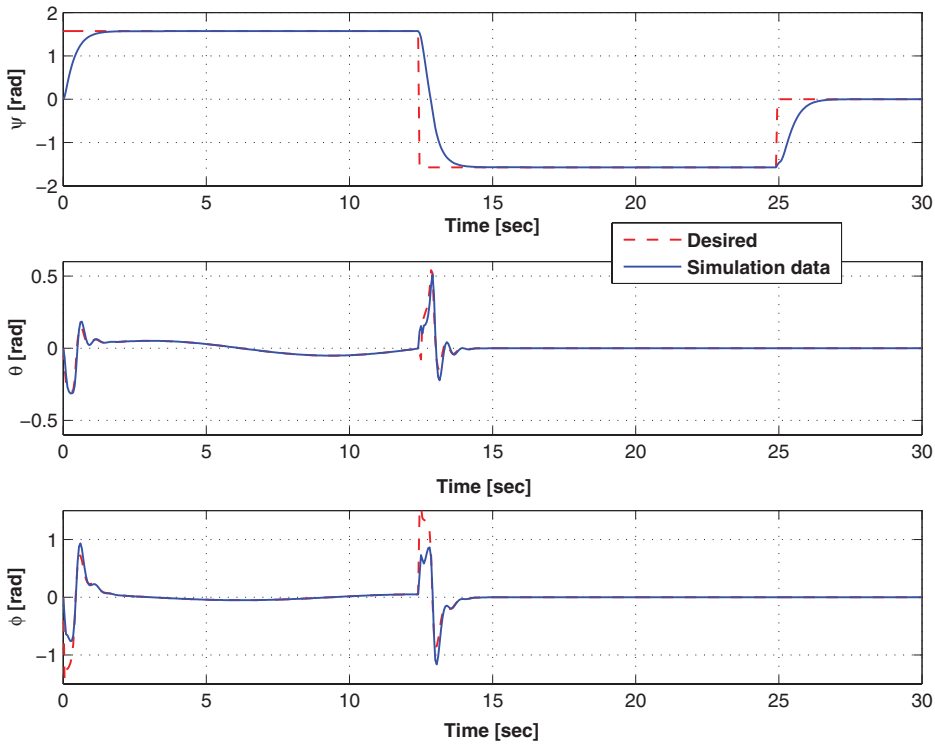

Fig. 4. (Colour online) Time evolution of attitude variables.

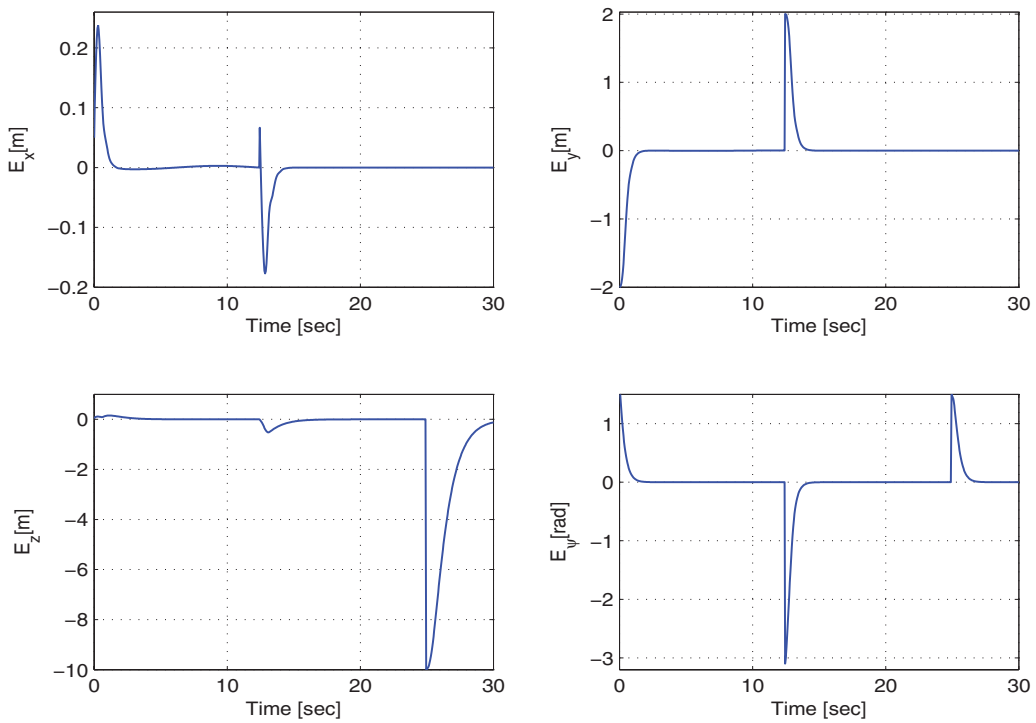

Fig. 5. (Colour online) Time evolution of pose errors.

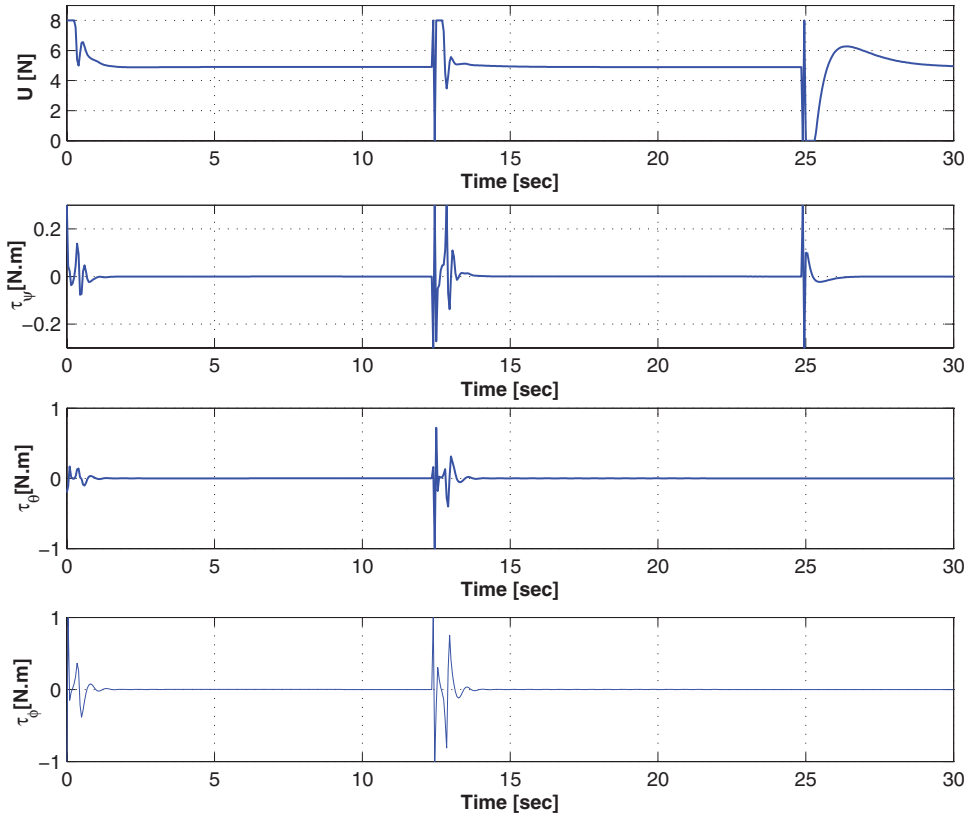

Fig. 6. (Colour online) Time evolution of control actions.

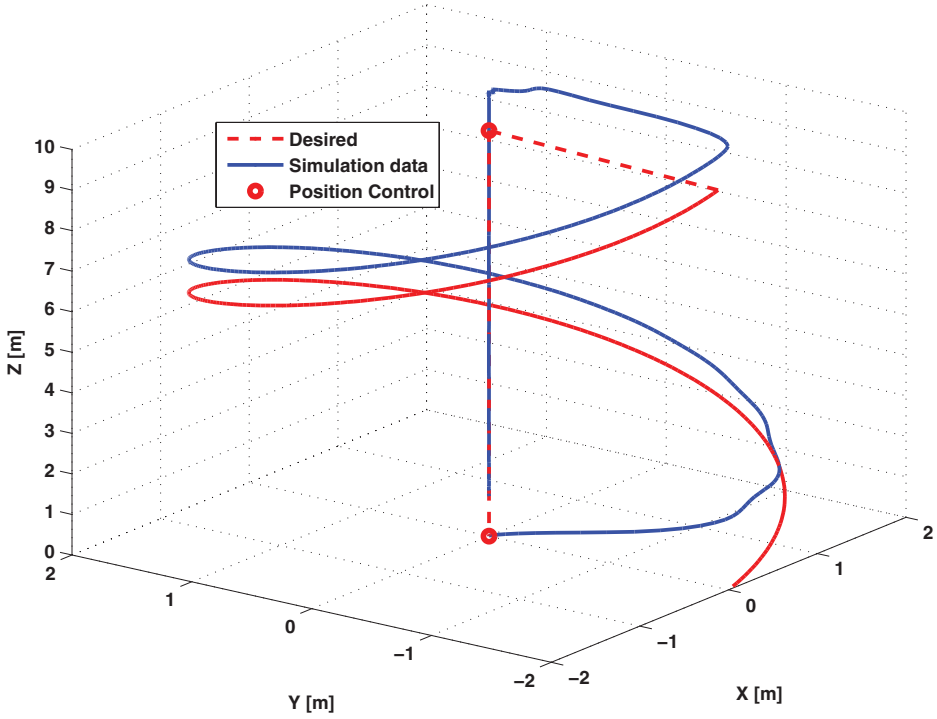

Fig. 7. (Colour online) Evolution of the quadrotor position with parametric uncertainties.

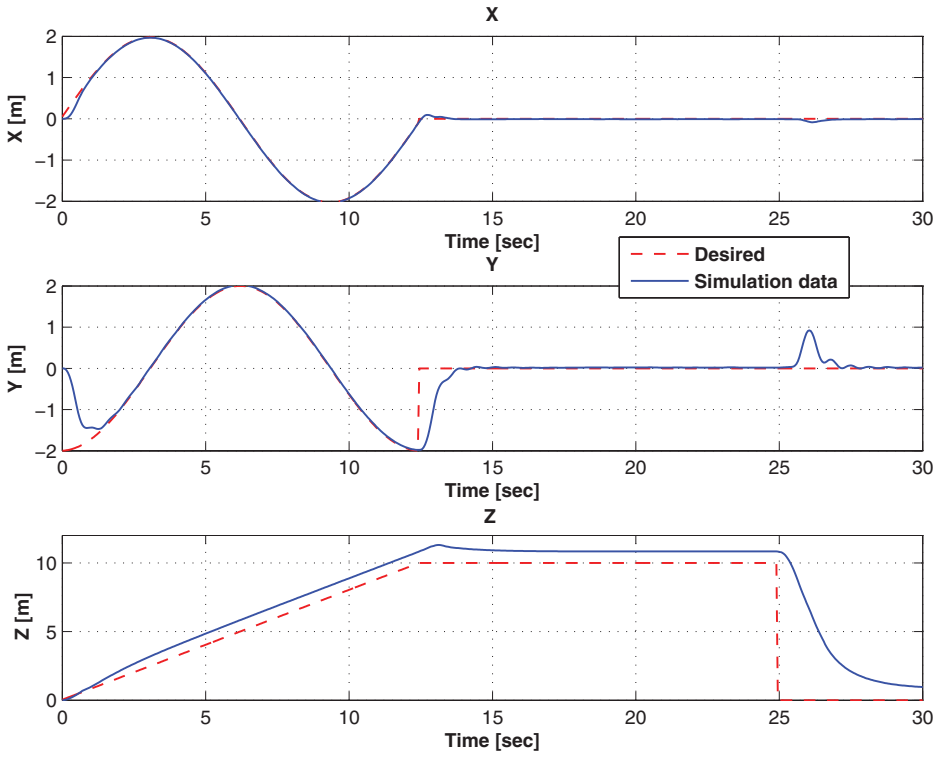

Fig. 8. (Colour online) Time evolution of position variables with parametric uncertainties and measurement noise.

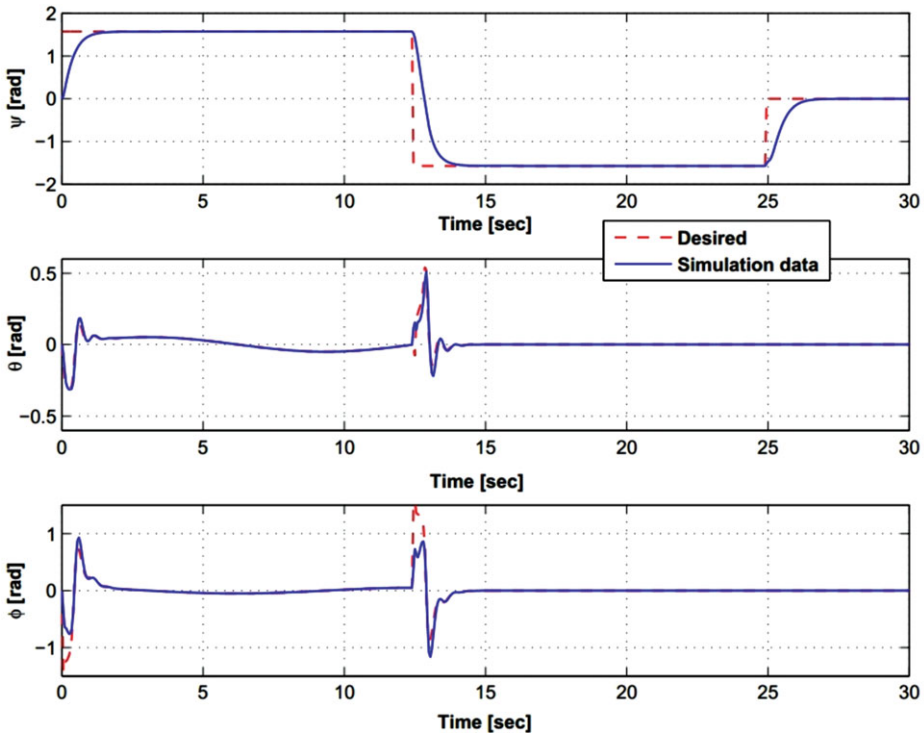

Fig. 9. (Colour online) Time evolution of pose errors with parametric uncertainties and measurement noise.

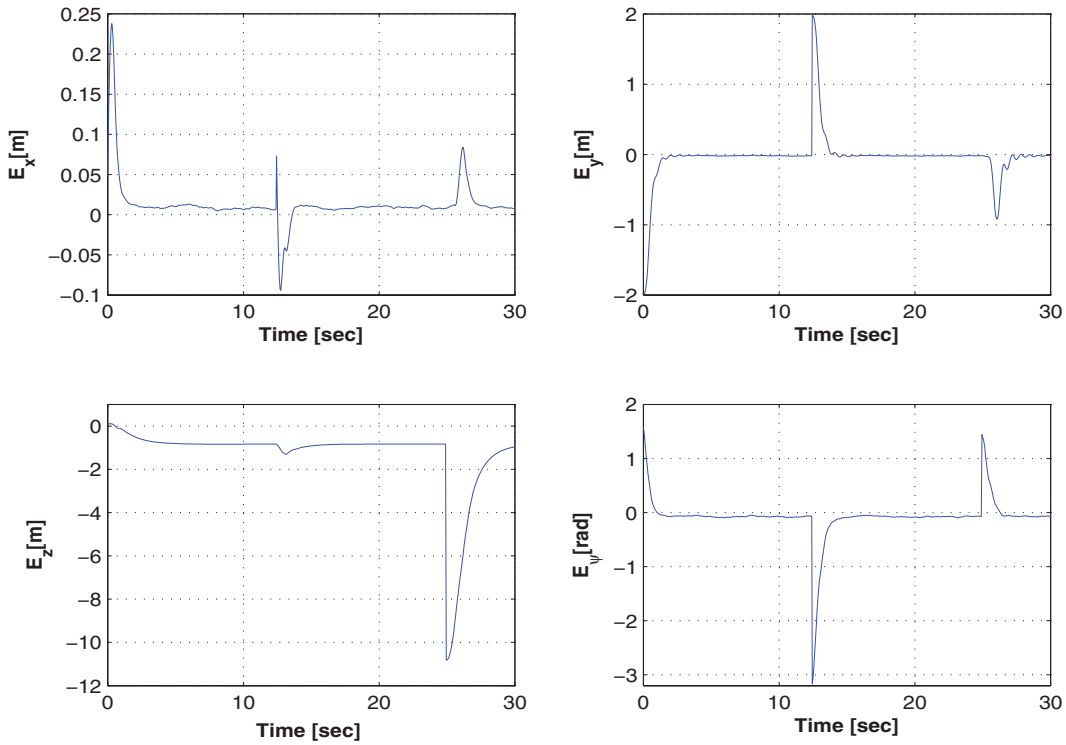

Fig. 10. (Colour online) Time evolution of pose errors with parametric uncertainties and measurement noise.

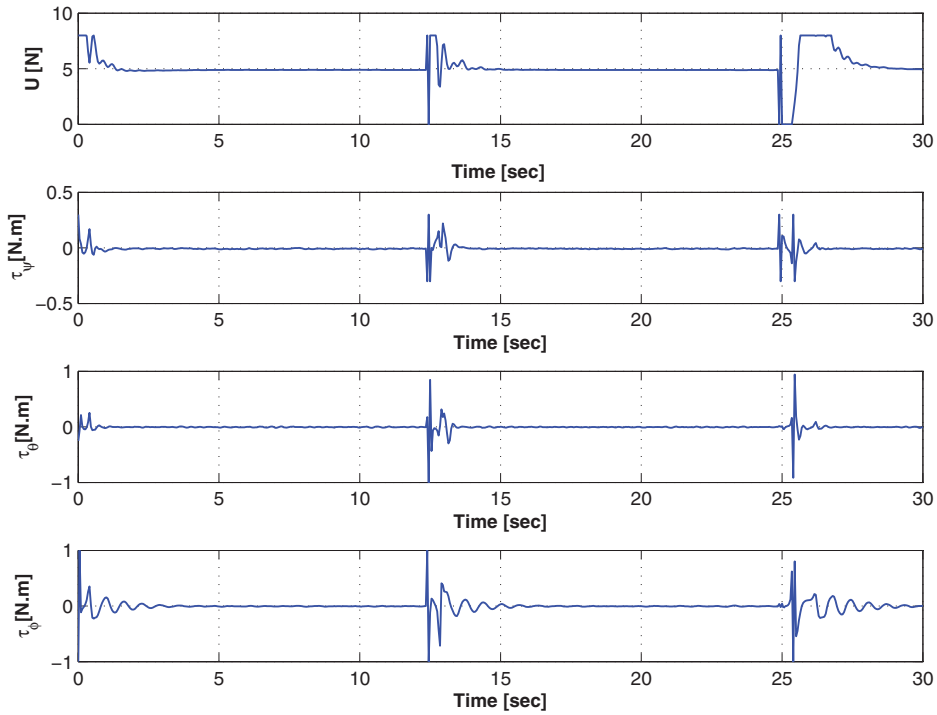

Fig. 11. (Colour online) Time evolution of control actions with parametric uncertainties and measurement noise.

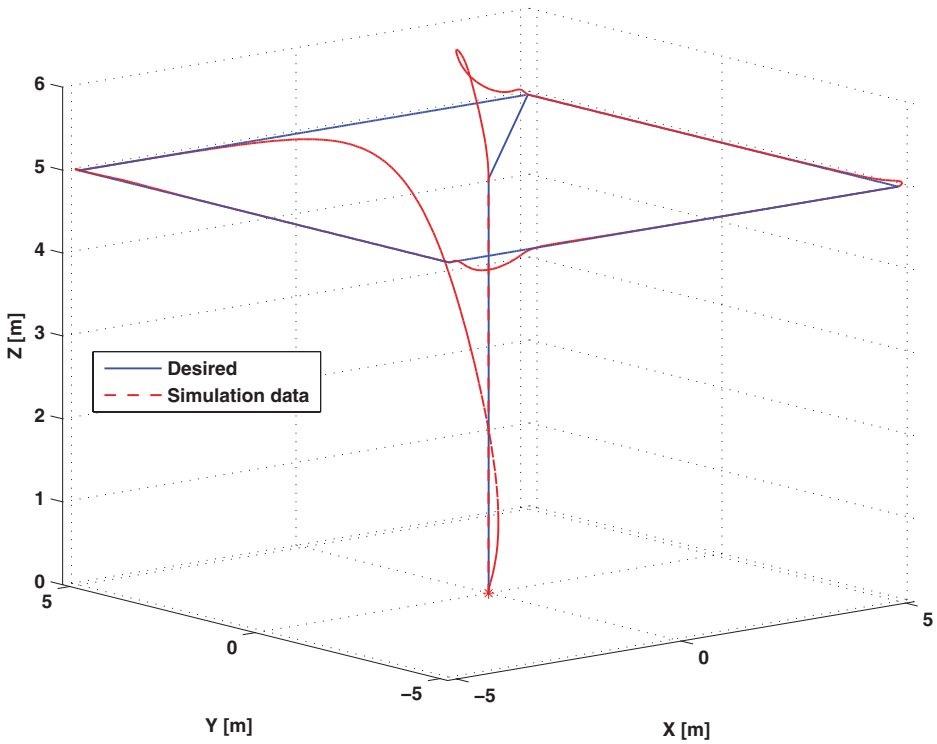

Fig. 12. (Colour online) Evolution of the quadrotor position for a square trajectory.

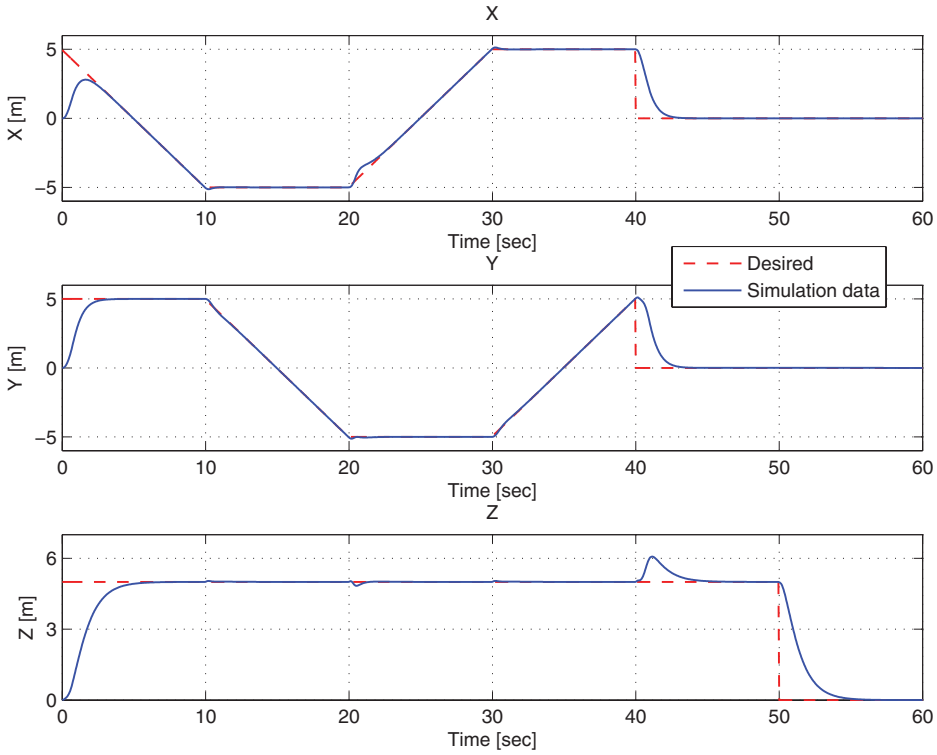

Fig. 13. (Colour online) Time evolution of position variables for a square trajectory.

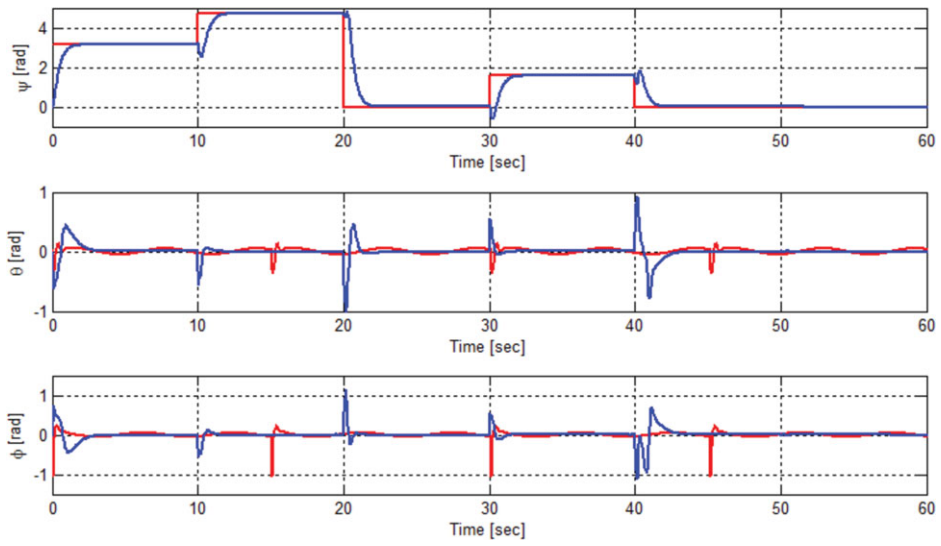

Fig. 14. (Colour online) Time evolution of pose errors for a square trajectory.

the condition imposed by real the physical system. Since the helicopter is an inertial system, it is impossible to follow the corners perfectly the trajectory, but rather, it approaches along a curved trajectory. Figures 12, 13, 14, 15 and 16 are the simulation of a square trajectory at constant height, showing that the controller can cope with square trajectories, where reference variations at corners are very abrupt, causing considerable control actions.

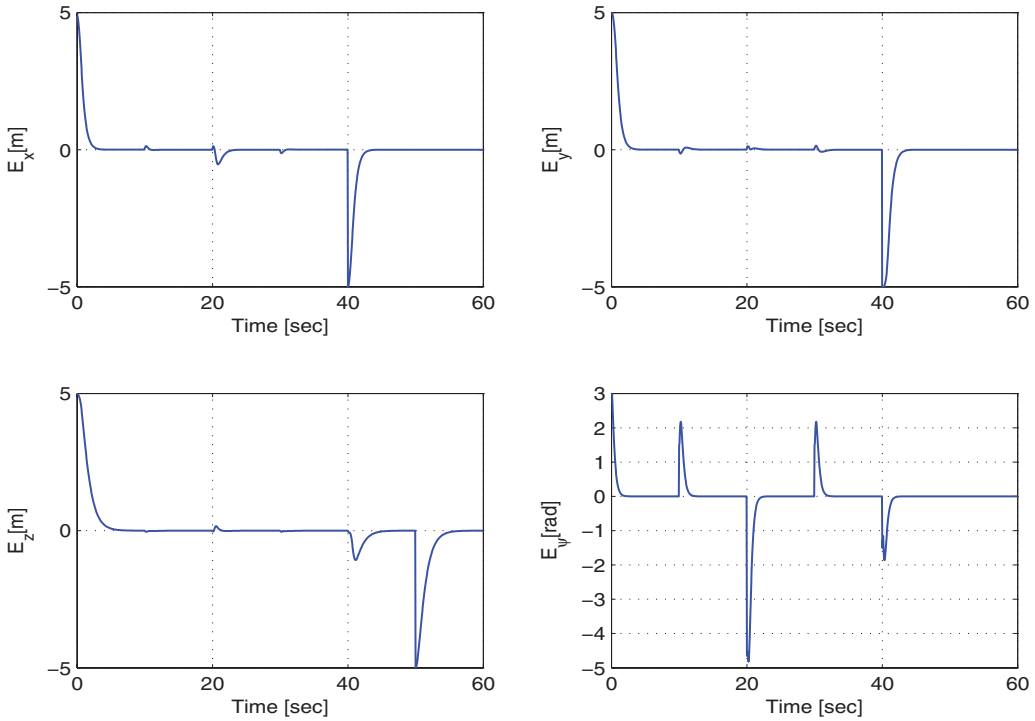

Fig. 15. (Colour online) Time evolution of pose errors for a square trajectory.

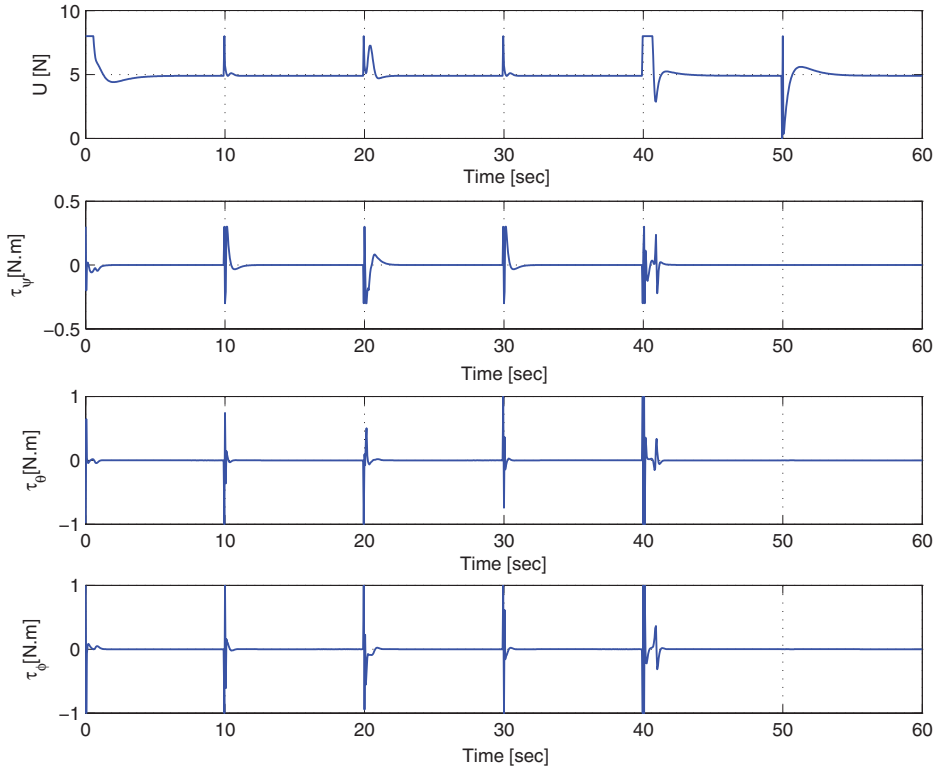

Fig. 16. (Colour online) Time evolution of control actions for a square trajectory.

5. Conclusions

This paper presents the design of a trajectory controller for a four-rotor mini helicopter. To this aim, an approximation of the helicopter's dynamic model using numerical methods is used. The proposed controller allows performing trajectory tracking as well as position control without switching the controller. In addition, the controller is easy to design and to implement with a minor computational complexity. Simulations have shown the good performance of the controller, even under parametric errors and measurement noise. The parameter that mainly affects the performance is aircraft's mass, but typically, this parameter is easily detected.

Future work will deal with extending the controller proposal to other unmanned aerial vehicles, and a systematic study on the robustness properties of the controller, as well as the analytical limitation of control actions to ensure its boundedness for any operation condition.

Acknowledgements

This work was partially supported by the Consejo Nacional de Investigaciones Científicas y Técnicas (CONICET), Argentina.

References

1. E. Altug, J.P. Ostrowski and C. Taylor, Quadrotor Control Using Dual Camera Visual Feedback," *IEEE International Conference on Robotics and Automation*, volume 3 (Sep. 14–19, 2003) pp. 4294–4299.
2. E. D. Beckmann and G. A. Borges, "Nonlinear Modeling, Identification and Control for a Simulated Miniature Helicopter," *IEEE Latin American Robotic Symposium*, Natal, Rio Grande do Norte, Brazil (Oct. 29–30, 2008) pp. 53–58.
3. A. Benallegue, A. Mokhtari and L. Fridman, "Feedback Linearization and High Order Sliding Mode Observer for a Quadrotor Uav," *International Workshop on Variable Structure Systems*, Alghero, Sardinia, Italy (Jun. 5–7, 2006) pp. 365–372.
4. M. Bernard, K. Kondak, N. Meyer, Y. Zhang and G. Hommel, "Elaborated Modeling and Control for an Autonomous Quad-Rotor," *22nd International Bristol UAV Systems Conference*, Bristol, UK (Apr. 16–18, 2007) pp. 27.1–27.10.
5. S. Bouabdallah, P. Murrieri and R. Siegwart, "Design and Control of an Indoor Micro Quadrotor," *IEEE International Conference on Robotic and Automation*, volume 5, New Orleans, LA, USA (Apr. 26–May 1, 2004) pp. 4393–4398.
6. S. Bouabdallah, A. Noth and R. Siegwart, "Pid vs lq Control Techniques Applied to an Indoor Micro Quadrotor," *IEEE/RSJ International Conference on Intelligent Robots and Systems.*, volume 3 (April 26–May 1, 2004) pp. 2451–2456.
7. P. Castillo, A. Dzul and R. Lozano, "Real-time stabilization and tracking of a four-rotor mini rotorcraft," *IEEE Trans. Control Syst. Technol.* **12**, 510–516 (Jul. 2004).
8. P. Castillo, R. Lozano and A. Dzul, *Modelling and Control of Mini-Flying Machines* (Springer, USA, 2005).
9. P. Castillo, R. Lozano and A. Dzul, "Stabilization of a mini rotorcraft with four rotors," *IEEE Control Syst. Mag.* **25**(6), 45–55 (Dec. 2005).
10. A. Das, F. Lewis and K. Subbarao, "Backstepping approach for controlling a quadrotor using lagrange form dynamics," *J. Intell. Robot. Syst.* **56**(1), 127–151 (2009).
11. L. Derafa, T. Madani and A. Benallegue, "Dynamic Modelling and Experimental Identification of Four Rotors Helicopter Parameters," *IEEE International Conference on Industrial Technology*, Mumbai, India (Dec. 15–17, 2006) pp. 1834–1839.
12. H. Eisenbeiss, "A Mini Unmanned Aerial Vehicle (Uav): System Overview and Image Acquisition," *International Workshop on Processing and Visualization Using High-Resolution Imagery*, volume 36, Pitsanulok, Thailand, (Nov. 18–20, 2004) pp. 1–7.
13. M. A. Hsieh, A. Cowley, J. F. Keller, L. Chaimowicz, B. Grocholsky, V. Kumar, C. J. Taylor, Y. Endo, Ronald C. Arkin, B. Jung, D. F. Wolf, G. S. Sukhatme and D. C. MacKenzie, "Adaptive teams of autonomous aerial and ground robots for situational awareness," *J. Field Robot.* **24**(11–12), 991–1014 (2007).
14. F. Kendoul, Z. Yu and K. Nonami, "Guidance and nonlinear control system for autonomous flight of minirotorcraft unmanned aerial vehicles," *J. Field Robot.* **27**(3), 311–334 (2010).
15. K. Kondak, M. Bernard, N. Meyer and G. Hommel, "Autonomously Flying Vtol-Robots: Modeling and Control," *IEEE International Conference on Robotics and Automation*, Rome, Italy (Apr. 10–14, 2007) pp. 736–741, .
16. L. Ma and Y. Chen, Aerial Surveillance System for Overhead Power Line Inspection, (Technical report, Center for Self-Organizing and Intelligent Systems (CSOIS) Department of Electrical and Computer Engineering College of Engineering, Utah State Universtiy USA, 2004).

17. T. Madani and A. Benallegue, "Control of a Quadrotor Mini-Helicopter Via Full State Backstepping Technique," *45th IEEE Conference on Decision and Control*, San Diego, CA, USA (Dec. 13–15, 2006) pp. 1515–1520.
18. I. Maza, F. Caballero, J. Capitán, J. Martínez de Dios and A. Ollero, "Experimental results in multi-uav coordination for disaster management and civil security applications," *J. Intell. Robot. Syst.* **64**(1–4), 563–585 (Dec. 2010).
19. N. Michael, J. Kink and V. Kumar, "Coopertative manipulation and transportation with aereal robots," *Autonumous Robots* **30**(1), 73–86 (Sep. 2010).
20. P. Pounds, J. Gresham, P. Corke and J. Roberts, "Towards Dynamically-Favourable Quad-Rotor Aerial Robots," *Australasian Conference on Robotics and Automation*, Canberra, Australia (Dec. 6–8, 2004).
21. P. Pounds, R. Mahony and P. Corke, "Modelling and Control of a Quad-Rotor Robot," *Australasian Conference on Robotics and Automation*, Auckland, New Zealand (Dec. 6–8, 2006).
22. G. V. Raffo, M. G. Ortega and F. R. Rubio, "An integral predictive/nonlinear $\mathcal{H}_\infty$ control structure for a quadrotor helicopter," *Automatica* **46**, 29–39 (2010).
23. A. Rosales, G. Scaglia and F. di Sciascio, "Formation control and trajectory tracking of mobile robotic systems - a linear algebra approach," *Robotica* **29**, 335–349 (2011).
24. A. Rosales, G. Scaglia, V. Mut and F. di Sciascio, "Trajectory tracking of mobile robots in dynamic environments - a linear algebra approach," *Robotica* **27**, 981–997 (2009).
25. G. Scaglia, L. Quintero Montoya, V. Mut and F. di Sciascio, "Numerical methods based controller design for mobile robots," *Robotica* **27**, 269–279 (2009).
26. G. Scaglia, A. Rosales, L. Quintero, V. Mut and R. Agarwal, "A linear-interpolation-based controller design for trajectory tracking of mobile robots," *Control Eng. Pract.* **18**, 318–329 (2010).
27. D. Schafroth, C. Bermes, S. Bouabdallah and R. Siegwart, "Modeling, system identification and robust control of a coaxial micro helicopter," *Control Eng. Pract.* **18**(7), 700–711 (Jul. 2010).
28. G. Strang, *Linear Algebra and its Application* (Academic Press., San Francisco, CA, USA, 1980).
29. H. Voos, "Nonlinear Control of a Quadrotor Micro-Uav using Feedback-Linearization," *IEEE International Conference on Mechatronics* (May 14–17, 2009) pp. 1–6.
30. S. L. Waslander, G. Hoffmann, J. S. Jang and C. J. Tomlin, "Multi-Agent x4-Flyer Testbed Design: Integral Sliding Mode vs. Reinforcement Learning," *IEEE/RSJ International Intelligent Robots and Systems (IROS 2005)*, Edmonton, AB, Canada (Aug. 2–6, 2005) pp. 6085–6090.

Appendix A

The controller design was made in discrete domain; therefore the stability analysis is developed in the same domain.[26] Consequently, it needs for a discretized version of the model helicopter. Considering the quadrotor behaviour described by (18), the model discretized through Euler approximation is stated in (23) and the designed controller by (39), (40), (41) and (42). Euler approximation is a usual discretization method showing reasonable certainty when the sampling time is short in relation to the vehicle dynamics.

By defining $e_{(n)}$ as the control error at time n-th ($e_{(n)} = [x_{d_{(n)}} - x_{(n)}, y_{d_{(n)}} - y_{(n)}, z_{d_{(n)}} - z_{(n)}, \psi_{d_{(n)}} - \psi_{(n)}]$), then, $\|e_n\| \to 0, n \to \infty$ when the positioning and trajectory tracking problems are considered.

The control actions (u, τ_ϕ, τ_θ,τ_ψ) are constant at every sampling time. By starting with the variable $x_{11} = \psi$, it may be considered independent for analysis, because it is not coupled to any other variable. Substituting (42) in to the corresponding equation of the system (23), the behavior of $x_{12} = \dot{\psi}$ can be analyzed.

$$\begin{aligned} x_{12_{(n+1)}} &= x_{12_{(n)}} + T_o \left(\frac{x_{12d(n+1)} - k_{x12}(x_{12d_{(n)}} - x_{12(n)}) - x_{12(n)}}{T_o} \right) \\ x_{12(n+1)} &- x_{12d_{(n+1)}} - k_{x12}(x_{12d_{(n)}} - x_{12(n)}) = 0 \\ ex_{12_{(n+1)}} &- k_{x12} ex_{12_{(n)}} = 0 \end{aligned} \tag{A.1}$$

If, $0 < k_{x12} < 1$, then $ex_{12(n+1)} \to 0$ when $n \to \infty$. The same procedure is applied to the $x_{11} = \psi$ angle.

$$x_{11_{(n+1)}} = x_{11_{(n)}} + T_o x_{12_{(n+1)}} = x_{11_{(n)}} + T_o(x_{12d_{(n+1)}} + ex_{12_{(n+1)}})$$

$$x_{11_{(n+1)}} = x_{11_{(n)}} + T_o x_{12d_{(n+1)}} + T_o ex_{12_{(n+1)}}$$

By replacing (32) in the above equation

$$\begin{aligned} x_{11_{(n+1)}} &= x_{11_{(n)}} + T_o\left(\frac{x_{11d_{(n+1)}} - k_{x11}(x_{11d_{(n)}} - x_{11_{(n)}})}{T_o}\right) + T_o ex_{12_{(n+1)}} \\ 0 &= x_{11d_{(n+1)}} - x_{11_{(n+1)}} - k_{x11}(x_{11d_{(n)}} - x_{11_{(n)}}) + T_o ex_{12_{(n+1)}} \\ 0 &= ex_{11_{(n+1)}} - k_{x11} ex_{11_{(n)}} + T_o ex_{12_{(n+1)}} \end{aligned} \tag{A.2}$$

If, $0 < k_{x11} < 1$ and as $ex_{12_{(n+1)}} \to 0$ with $n \to \infty \Rightarrow ex_{11_{(n+1)}} \to 0$ with $n \to \infty$.

It demonstrates that the reference angle ψ_d is being tracked. The analysis is equally applied to ϕ and θ; therefore, it is omitted from this demonstration and the conclusions are alike, $ex_{10_{(n+1)}} \to 0$ with $n \to \infty \Rightarrow ex_{9_{(n+1)}} \to 0$ with $n \to \infty$ and $ex_{8_{(n+1)}} \to 0$ with $n \to \infty \Rightarrow ex_{7_{(n+1)}} \to 0$ whit $n \to \infty$. The analysis for other variables is made below.

The next variable is x_6, which represents the speed on z axis. From the corresponding system Eq. (23)

$$x_{6_{(n+1)}} = x_{6_{(n)}} + \frac{u_{(n)} T_o}{m} \cos x_{9_{(n+1)}} \cos x_{7_{(n+1)}} - g T_o \tag{A.3}$$

Let us define the Taylor's series of first order for a multi-variable function,

$$F_{(x,y)} = F_{(a,b)} + R_{n_{(F)}} = F_{(a,b)} + \frac{\partial F_{(c)}}{\partial x}(x - a) + \frac{\partial F_{(c)}}{\partial y}(y - a) \tag{A.4}$$

where $(x, y) < c < (a, b)$. And applying (A.4) in (A.3),

$$\begin{aligned} \cos x_{9_{(n+1)}} \cos x_{7_{(n+1)}} = {} & \cos x_{9d_{(n+1)}} \cos x_{7d_{(n+1)}} + (x_{9_{(n+1)}} - x_{9d_{(n+1)}}) \cdot \\ & \cdot \left[-\sin(x_{9d_{(n+1)}} + \Theta(x_{9d_{(n+1)}} - x_{9_{(n+1)}}))\right] \cos(x_{7d_{(n+1)}} + \Theta(x_{7d_{(n+1)}} - x_{7_{(n+1)}})) \\ & + (x_{7_{(n+1)}} - x_{7d_{(n+1)}}) \cos(x_{9_{(n+1)}} + \Theta(x_{9d_{(n+1)}} - x_{9_{(n+1)}})) \cdot \\ & \cdot \left[-\sin(x_{7d_{(n+1)}} + \Theta(x_{7d_{(n+1)}} - x_{7_{(n+1)}}))\right] \end{aligned} \tag{A.5}$$

where $0 < \Theta < 1$. Also, let us define $ex_{7_{(n+1)}} = (x_{7d_{(n+1)}} - x_{7_{(n+1)}})$, $ex_{9_{(n+1)}} = (x_{9d_{(n+1)}} - x_{9_{(n+1)}})$, $f_1 = [-\sin(x_{9d_{(n+1)}} + \Theta(x_{9d_{(n+1)}} - x_{9_{(n+1)}}))] \cos(x_{7d_{(n+1)}} + \Theta(x_{7d_{(n+1)}} - x_{7_{(n+1)}}))$ and $f_2 = \cos(x_{9_{(n+1)}} + \Theta(x_{9d_{(n+1)}} - x_{9_{(n+1)}}))[-\sin(x_{7d_{(n+1)}} + \Theta(x_{7d_{(n+1)}} - x_{7_{(n+1)}}))]$; and substituting all these in the previous equation

$$x_{6_{(n+1)}} = x_{6_{(n)}} + \frac{u_{(n)} T_o}{m}\left[\cos x_{9d_{(n+1)}} \cos x_{7d_{(n+1)}} - f_1 ex_{9_{(n+1)}} - f_2 ex_{7_{(n+1)}}\right] - g T_o \tag{A.6}$$

From (28) and (29),

$$\begin{aligned} \Delta x_4 &= \frac{\sin x_{7d_{(n+1)}}}{\cos x_{7d_{(n+1)}}}(\Delta x_6 + g T_o) \\ -\Delta x_2 &= \frac{\Delta x_4 \sin x_{9d_{(n+1)}}}{\sin x_{7d_{(n+1)}} \cos x_{9d_{(n+1)}}} = \frac{\sin x_{9d_{(n+1)}}(\Delta x_6 + g T_o)}{\cos x_{7d_{(n+1)}} \cos x_{9d_{(n+1)}}} \end{aligned} \tag{A.7}$$

and substituting (A.7) in the definition of the control action stated in (39).

$$u_{(n)} = \frac{m}{T_o}(\Delta x_6 + gT_o)\left[\frac{\sin^2 x_{9d_{(n+1)}}}{\cos x_{7d_{(n+1)}}\cos x_{9d_{(n+1)}}} + \frac{\sin^2 x_{7d_{(n+1)}}\cos x_{9d_{(n+1)}}}{\cos x_{7d_{(n+1)}}} + \cos x_{7d_{(n+1)}}\cos x_{9d_{(n+1)}}\right]$$

$$u_{(n)} = \frac{m}{T_o}(\Delta x_6 + gT_o)\left[\frac{\sin^2 x_{9d_{(n+1)}} + \sin^2 x_{7d_{(n+1)}}\cos^2 x_{9d_{(n+1)}} + \cos^2 x_{7d_{(n+1)}}\cos^2 x_{9d_{(n+1)}}}{\cos x_{7d_{(n+1)}}\cos x_{9d_{(n+1)}}}\right]$$

$$u_{(n)} = \frac{m}{T_o}(\Delta x_6 + gT_o)\frac{1}{\cos x_{7d_{(n+1)}}\cos x_{9d_{(n+1)}}} \tag{A.8}$$

Then, replacing (A.8) into (A.6)

$$\begin{aligned} x_{6_{(n+1)}} = x_{6_{(n)}} + \frac{m}{T_o}(\Delta x_6 + gT_o)\frac{1}{\cos x_{7d_{(n+1)}}\cos x_{9d_{(n+1)}}}\frac{T_o}{m}\cos x_{7d_{(n+1)}}\cos x_{9d_{(n+1)}} \\ - gT_o + \frac{u_{(n)}T_o}{m}(-f_1 ex_{7_{(n+1)}} - f_2 ex_{9_{(n+1)}}) \end{aligned} \tag{A.9}$$

Also substituting Δx_6 by its expression given in (31) and (34),

$$\begin{aligned} x_{6_{(n+1)}} &= x_{6_{(n)}} + x_{6ref_{(n+1)}} - k_{x6}(x_{6ref_{(n)}} - x_{6_{(n)}}) - x_{6_{(n)}} + \frac{u_{(n)}T_o}{m}(f_1 ex_{7_{(n+1)}} + f_2 ex_{9_{(n+1)}}) \\ ex_{6_{(n+1)}} &= k_{x6} ex_{6_{(n)}} - \frac{u_{(n)}T_o}{m}(f_1 ex_{7_{(n+1)}} + f_2 ex_{9_{(n+1)}}) \end{aligned} \tag{A.10}$$

Equation (A.10) represents a lineal system and a nonlinearity which tends to 0 because $ex_{7(n+1)}$ and $ex_{9(n+1)} \to 0$ whit $n \to \infty$.

The same analysis applies for x_4. From (23),

$$x_{4_{(n+1)}} = x_{4_{(n)}} + \frac{u_{(n)}T_o}{m}\cos x_{9_{(n+1)}}\sin x_{7_{(n+1)}} \tag{A.11}$$

By applying (A.4) into (A.11),

$$\begin{aligned} \cos x_{9_{(n+1)}}\sin x_{7_{(n+1)}} = \cos x_{9d_{(n+1)}}\sin x_{7d_{(n+1)}} + [x_{9_{(n+1)}} - x_{9d_{(n+1)}}]\cdot \\ \cdot[-\sin(x_{9_{(n+1)}} + \zeta(x_{9d_{(n+1)}} - x_{9_{(n+1)}}))][\sin(x_{7_{(n+1)}} + \zeta(x_{7d_{(n+1)}} - x_{7_{(n+1)}}))] \\ + [x_{7_{(n+1)}} - x_{7d_{(n+1)}}]\cos(x_{9_{(n+1)}} + \zeta(x_{9d_{(n+1)}} - x_{9_{(n+1)}}))\cdot \\ \cdot \cos(x_{7_{(n+1)}} + \zeta(x_{7d_{(n+1)}} - x_{7_{(n+1)}})) \end{aligned} \tag{A.12}$$

where $0 < \zeta < 1$ let's define $ex_{7_{(n+1)}} = (x_{7d_{(n+1)}} - x_{7_{(n+1)}})$, $ex_{9_{(n+1)}} = (x_{9_{(n+1)}} - x_{9d_{(n+1)}})$, $h_1 = \cos(x_{9_{(n+1)}} + \zeta(x_{9d_{(n+1)}} - x_{9_{(n+1)}}))\cos(x_{7_{(n+1)}} + \zeta(x_{7_{(n+1)}} - x_{7_{(n+1)}}))$ and $h_2 = [-\sin(x_{9_{(n+1)}} + \zeta(x_{9d_{(n+1)}} - x_{9_{(n+1)}}))][\sin(x_{7_{(n+1)}} + \zeta(x_{7d_{(n+1)}} - x_{7_{(n+1)}}))$, and substituting all this in the previous equation.

$$\cos x_{9_{(n+1)}}\sin x_{7_{(n+1)}} = \cos x_{9d_{(n+1)}}\sin x_{7d_{(n+1)}} + h_1 ex_{7_{(n+1)}} + h_2 ex_{9_{(n+1)}} \tag{A.13}$$

By replacing (A.13) into (A.11),

$$x_{4_{(n+1)}} = x_{4_{(n)}} + \frac{u_{(n)}T_o}{m}\cos x_{9d_{(n+1)}}\sin x_{7d_{(n+1)}} + \frac{u_{(n)}T_o}{m}[h_1 ex_{7_{(n+1)}} + h_2 ex_{9_{(n+1)}}] \tag{A.14}$$

From (28) and (29) the following relations are obtained,

$$-\Delta x_2 = \frac{\Delta x_4 \sin x_{9d_{(n+1)}}}{\cos x_{9d_{(n+1)}} \sin x_{7d_{(n+1)}}} \tag{A.15}$$

$$\Delta x_6 + gT_o = \Delta x_4 \frac{\cos x_{7d_{(n+1)}}}{\sin x_{7d_{(n+1)}}} \tag{A.16}$$

By substituting (A.15) in the control action u defined in (39),

$$u_{(n)} = \frac{m}{T_o}\left[\frac{\Delta x_4 \sin^2 x_{9d_{(n+1)}}}{\cos x_{9d_{(n+1)}} \sin x_{7d_{(n+1)}}} + \Delta x_4 \cos x_{9d_{(n+1)}} \sin x_{7d_{(n+1)}} + \Delta x_4 \frac{\cos^2 x_{7d_{(n+1)}}}{\sin x_{7d_{(n+1)}}} \cos x_{9d_{(n+1)}}\right]$$

$$u_{(n)} = \frac{m\Delta x_4}{T_o}\left[\frac{\sin^2 x_{9d_{(n+1)}} + \cos^2 x_{9d_{(n+1)}} \sin^2 x_{7d_{(n+1)}} + \cos^2 x_{7d_{(n+1)}} \cos^2 x_{9d_{(n+1)}}}{\cos x_{9d_{(n+1)}} \sin x_{7d_{(n+1)}}}\right] \tag{A.17}$$

$$u_{(n)} = \frac{m\Delta x_4}{T_o} \frac{1}{\cos x_{9d_{(n+1)}} \sin x_{7d_{(n+1)}}}$$

Now, (A.17) into (A.14)

$$x_{4_{(n+1)}} = x_{4_{(n)}} + \frac{m\Delta x_4}{T_o} \frac{1}{\cos x_{9d_{(n+1)}} \sin x_{7d_{(n+1)}}} \frac{T_o}{m} \cos x_{9d_{(n+1)}} \sin x_{7d_{(n+1)}}$$

$$+ \frac{u_{(n)} T_o}{m}[h_1 ex_{7_{(n+1)}} + h_2 ex_{9_{(n+1)}}] \tag{A.18}$$

From (31) and (34), the following expression is found

$$x_{4(n+1)} = x_{4(n)} + x_{4ref(n+1)} - k_{x4}(x_{4ref(n)} - x_{4(n)}) - x_{4(n)} + \frac{u_{(n)} T_o}{m}[h_1 ex_{7(n+1)} + h_2 ex_{9(n+1)}]$$

$$ex_{4_{(n+1)}} = k_{x4} ex_{4_{(n)}} - u_{(n)} \frac{T_o}{m}[h_1 ex_{7_{(n+1)}} + h_2 ex_{9_{(n+1)}}] \tag{A.19}$$

Equation (A.19) represents a lineal system and a nonlinearity which tends to 0 because $ex_{7(n+1)}$ and $ex_{9_{(n+1)}} \to 0$ whit $n \to \infty$.

Finally we discuss x_2 likewise that previous cases. From (23)

$$x_{2_{(n+1)}} = x_{2_{(n)}} - \frac{u_{(n)} T_o}{m} \sin x_{9_{(n+1)}} \tag{A.20}$$

and applying (A.4) into (A.20),

$$\sin x_{9_{(n+1)}} = \sin x_{9d_{(n+1)}} + \cos(x_{9d_{(n+1)}} + \varrho(x_{9_{(n+1)}} - x_{9d_{(n+1)}}))(x_{9_{(n+1)}} - x_{9d_{(n+1)}}) \tag{A.21}$$

where $0 < \varrho < 1$ and also define $ex_{9_{(n+1)}} = (x_{9_{(n+1)}} - x_{9d_{(n+1)}})$ and $g_1 = \cos(x_{9d_{(n+1)}} + \varrho(x_{9_{(n+1)}} - x_{9d_{(n+1)}}))$. Substituting into (A.20),

$$x_{2_{(n+1)}} = x_{2_{(n)}} - \frac{u_{(n)} T_o}{m}\left[\sin x_{9d_{(n+1)}} - g_1 ex_{9_{(n+1)}}\right] \tag{A.22}$$

From (28) and (29),

$$\Delta x_4 = -\Delta x_2 \frac{\sin x_{7d_{(n+1)}} \cos x_{9d_{(n+1)}}}{\sin x_{9d_{(n+1)}}}$$

$$\Delta x_6 + gT_o = \Delta x_4 \frac{\cos x_{7d_{(n+1)}}}{\sin x_{7d_{(n+1)}}} = -\Delta x_2 \frac{\cos x_{9d_{(n+1)}} \cos x_{7d_{(n+1)}}}{\sin x_{9d_{(n+1)}}} \tag{A.23}$$

Also, replacing (A.23) the expression of the control action $u_{(n)}$ given by (39) is obtained,

$$u_{(n)} = \frac{m}{T_o}\left[-\Delta x_2 \sin x_{9d_{(n+1)}} - \frac{\Delta x_2 \sin^2 x_{7d_{(n+1)}} \cos^2 x_{9d_{(n+1)}}}{\sin x_{9d_{(n+1)}}} - \frac{\Delta x_2 \cos^2 x_{9d_{(n+1)}} \cos^2 x_{7d_{(n+1)}}}{\sin x_{9d_{(n+1)}}}\right]$$

$$u_{(n)} = \frac{m\Delta x_2}{T_o}\left[\frac{-\sin^2 x_{9d_{(n+1)}} - \sin^2 x_{7d_{(n+1)}} \cos^2 x_{9d_{(n+1)}} - \cos^2 x_{7d_{(n+1)}} \cos^2 x_{9d_{(n+1)}}}{\sin x_{9d_{(n+1)}}}\right]$$

$$u_{(n)} = -\frac{m}{T_o}\frac{\Delta x_2}{\sin x_{9d_{(n+1)}}} \tag{A.24}$$

Replacing (A.24) into (A.22),

$$x_{2_{(n+1)}} = x_{2_{(n)}} + \frac{m}{T_o}\frac{\Delta x_2}{\sin x_{9d_{(n+1)}}}\frac{T_o}{m}\sin x_{9d_{(n+1)}} + u_{(n)}\frac{T_o}{m}g_1 ex9_{(n+1)}$$

$$x_{2_{(n+1)}} = x_{2_{(n)}} + \Delta x_2 + u_{(n)}\frac{T_o}{m}g_1 ex9_{(n+1)} \tag{A.25}$$

And substituting Δx_2 defined by (31) and (34) into (A.25), the following expressions attained,

$$x_{2_{(n+1)}} = x_{2_{(n)}} + x_{2ref} - k_2(x_{2ref_{(n)}} - x_{2_{(n)}}) - x_{2_{(n)}} + u_{(n)}\frac{T_o}{m}g_1 ex9_{(n+1)}$$

$$ex2_{(n+1)} = k_2 ex2_{(n)} - u_{(n)}\frac{T_o}{m}g_1 ex9_{(n+1)} \tag{A.26}$$

Equation (A.26) represents a lineal system and a nonlinearity which tends to 0 because $ex9_{(n+1)} \to 0$ with $n \to \infty$.

Recalling expressions (A.10), (A.19) and (A.26).

$$\begin{bmatrix} ex2_{(n+1)} \\ ex4_{(n+1)} \\ ex6_{(n+1)} \end{bmatrix} = \underbrace{\begin{bmatrix} k_{x2} & 0 & 0 \\ 0 & k_{x4} & 0 \\ 0 & 0 & k_{x6} \end{bmatrix}\begin{bmatrix} ex2_{(n)} \\ ex4_{(n)} \\ ex6_{(n)} \end{bmatrix}}_{Linear\ system} + \underbrace{\frac{u_{(n)}T_o}{m}\begin{bmatrix} -g_1 & 0 \\ h_1 & h_2 \\ f_1 & f_2 \end{bmatrix}\begin{bmatrix} ex9_{(n+1)} \\ ex7_{(n+1)} \end{bmatrix}}_{Nonlinearity} \tag{A.27}$$

Equation (A.27) represents a linear system and a nonlinearity which tends to zero because $ex7_{(n+1)}$ and $ex9_{(n+1)} \to 0$ with $n \to 0$. Finally, since $0 < k_{x2}, k_{x4}, k_{x6} < 1$ and $ex7_{(n+1)}$ and $ex9_{(n+1)} \to 0$ with $n \to 0$, it is demonstrated that $ex2_{(n+1)}$, $ex4_{(n+1)}$ and $ex6_{(n+1)} \to 0$ with $n \to \infty$.

Up to this point, it was shown that speed tracking errors ($ex2_{(n+1)}$, $ex4_{(n+1)}$, $ex6_{n+1}$) tend to 0 with $n \to \infty$, and that (A.2) has already proven that the yaw tracking error ($ex11_{(n+1)}$) $\to 0$ with $n \to \infty$. Only the trajectory tracking errors ($ex1_{(n+1)}$, $ex3_{(n+1)}$, $ex5_{(n+1)}$) remain to be analyzed and verified that they tend to zero with $n \to \infty$. From (23),

$$x_{1_{(n+1)}} = x_{1_{(n)}} + T_o x_{2_{(n+1)}} = x_{1_{(n)}} + T_o(x_{2d_{(n+1)}} + ex2_{(n+1)})$$

$$x_{1_{(n+1)}} = x_{1_{(n)}} + T_o x_{2d_{(n+1)}} + T_o ex2_{(n+1)}$$

By replacing $x_{2ref(n+1)}$ for its expression of (31),

$$x_{1_{(n+1)}} = x_{1_{(n)}} + T_o \frac{(x_{1ref_{(n+1)}} - k_{x1}(x_{1ref_{(n)}} - x_{1_{(n)}})) - x_{1_{(n)}}}{T_o} + Toex_{2_{(n+1)}} \tag{A.28}$$

With a like analysis as for x_3 and x_5, the following expressions are obtained,

$$ex_{1_{(n+1)}} = k_{x1} ex_{1_{(n)}} - T_o ex_{2_{(n+1)}} \tag{A.29}$$

$$ex_{3_{(n+1)}} = k_{x3} ex_{3_{(n)}} - T_o ex_{4_{(n+1)}} \tag{A.30}$$

$$ex_{5_{(n+1)}} = k_{x5} ex_{5_{(n)}} - T_o ex_{6_{(n+1)}} \tag{A.31}$$

Because $ex_{2_{(n+1)}}$, $ex_{4_{(n+1)}}$ and $ex_{6_{(n+1)}} \to 0$ with $n \to \infty$. It is finally prove that $ex_{1_{(n)}}$, $ex_{3_{(n)}}$ and $ex_{5_{(n)}} \to 0$ with $n \to \infty$, and the tracking error tends to 0.